

We are IntechOpen, the world's leading publisher of Open Access books Built by scientists, for scientists

6,900

Open access books available

185,000

International authors and editors

200M

Downloads

Our authors are among the

154

Countries delivered to

TOP 1%

most cited scientists

12.2%

Contributors from top 500 universities



WEB OF SCIENCE™

Selection of our books indexed in the Book Citation Index
in Web of Science™ Core Collection (BKCI)

Interested in publishing with us?
Contact book.department@intechopen.com

Numbers displayed above are based on latest data collected.
For more information visit www.intechopen.com



Dynamics of the Changjiang River Plume

Hui Wu, Tianning Wu, Jian Shen and Jianrong Zhu

Additional information is available at the end of the chapter

<http://dx.doi.org/10.5772/intechopen.80734>

Abstract

The extension of the Changjiang River plume is one of the fundamental processes in the Yellow and East China Seas, which is responsible not only for the physical properties of seawater but also for the numerous physical, biogeochemical, and sedimentary processes in this region. The studies of the Changjiang River plume dated back to 1960s, followed by generations, and are still attracting numerous focuses nowadays. Here in this chapter, we will review the past studies on the Changjiang River plume and present some latest studies on this massive river plume. The latest research progresses on the Changjiang River plume are mainly related to the tidal modulation mechanisms. It is found that the tide shifts the Changjiang River plume to the northeast outside the river mouth, bifurcates the plume at the head of submarine canyon, and arrests the unreal up-shelf plume intrusion that occurred frequently in previous model studies. It is also found that the tidal residual current transports part of the Changjiang River plume to the Subei Coastal Water. These tidal modulation effects can answer the questions on the dynamics of Changjiang River plume that puzzled the research community for decades.

Keywords: river plume dynamics, tide, up-shelf extension, numerical simulation, Changjiang River Estuary

1. Introduction

The Changjiang River, 6300 km long, drainage basin of 1.8 million km² and annual discharge of 9.32×10^{11} m³, is the largest river entering the western Pacific Ocean. It empties 51% freshwater, 23% sediments, 66% nitrogen, and 84% phosphorus of the total riverine fluxes in China, respectively [38, 44, 53] (**Figure 1**). Consequently, the Changjiang River Estuary (CRE) is one major fishery ground of China, but the excess nutrients and pollution inputs also have caused severe eutrophication, harmful algal blooms (HAB), and hypoxia [25, 42, 45, 64].

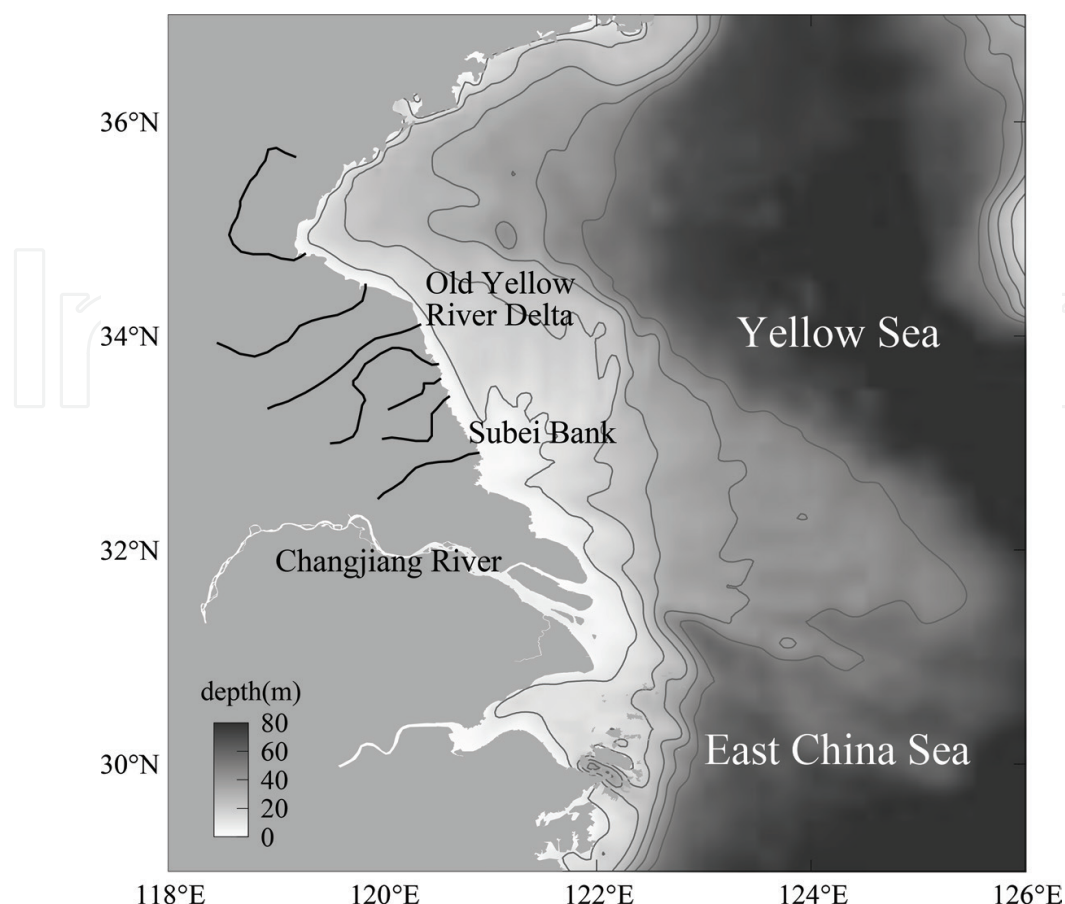


Figure 1. Topography of the Changjiang River Estuary and Subei Coastal Water.

North of the CRE is the most turbid coastal water in the East Asian marginal seas, that is, the Subei Coastal Water (SCW), which receives the Old Yellow River discharge in 1128–1855 [11, 58]. The SCW is well known for its unique radial tidal ridge system [15, 28] and frequent macroalgal blooms [29]. The extension of the Changjiang River plume substantially controls the distributions of sediments and nutrients in the Yellow and East China Seas (YECS) and determines the physical properties of water mass such as salinity and stratification, therefore is responsible for the occurrence of HABs and hypoxia. It also significantly influences the water mass composition in the SCW, as indicated by some recent studies (e.g., [50]). The CRE-SCW represents a rare type of coastal water body, which is coinfluenced by huge river discharges, energetic tides, strong shelf circulations, and the seasonal monsoon. Therefore, the behavior of the Changjiang River plume is complicated, which has attracted numerous research efforts in the past 60 years.

2. A research history voyage on the Changjiang River plume

Prof. Hanli Mao and his colleagues made the earliest study on the Changjiang River plume [30]. By analyzing the hydrological data obtained in the vicinity of the Changjiang River Estuary, they found that the Changjiang River plume extends southward along the Zhejiang

and Fujian Coast in winter season but northeastward toward the Jeju Island in summer season (**Figure 2**). Such a bi-directional plume extension was confirmed later by numerous studies, such as Beardsley [4] and Zhao et al. [60], among many others. The northeastward plume extension in summer is an iconic hydrodynamic feature in the Yellow and East China Seas, which directly causes the harmful algal blooming and hypoxia off the Changjiang River Estuary, by fueling the nutrients and forming the stratification [25, 64]. This offshore plume branch finally reaches the vicinity of the Jeju Island and further enters the Japan/East Sea through the Tsushima-Korea Strait [6, 21].

It has become a major oceanographic research topic to find the dynamic mechanisms responsible for the northeastward extension of the summertime Changjiang River plume. The wind direction in summer is southerly, which could favor an offshore extension under the surface Ekman transport. However, the observed northeastward plume extensions were not always

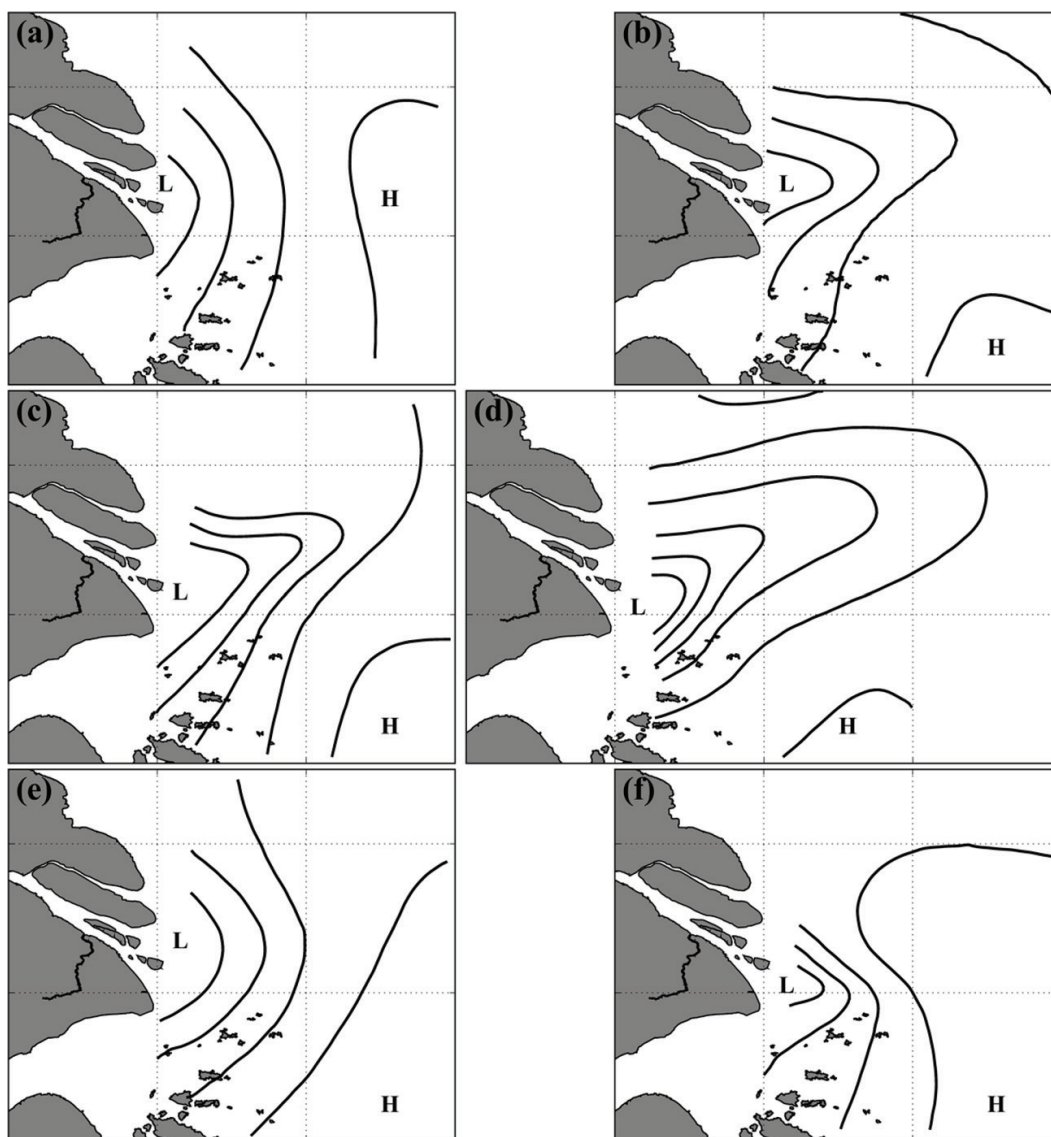


Figure 2. Distribution of the Changjiang River plume in April (a), May (b), June (c), July (d), August (e), and September (f). “L” means low salinity water; “H” means high salinity water. Replotted from Mao et al. [30].

associated with an upwelling-favorable southerly wind [60]. Some theoretical studies indicated that the magnitude of wind-driven current is too small to change the plume extension direction [23, 30]. In summer, the mean wind speed is $<3 \text{ m s}^{-1}$ and is generally weak, except during the typhoon weather. These studies suggested that a large Changjiang River runoff could be a prerequisite and proposed a “critical discharge” ($\sim 40,000 \text{ m}^3 \text{ s}^{-1}$), beyond which the northeastward extension should occur [3, 23, 30]. However, in many years with large runoff, the northeastward extension was actually absent; whereas, in some other years with low runoff, it was still observed [36, 57, 60]. Some studies speculated that the northward-flowing Taiwan warm current played a role in the northeastward plume extension, through the barotropic [60] or baroclinic [35] effects.

Since 1990s, with the growing computer power and the advances of numerical methods, researchers began to use three-dimensional numerical models to study the extension of Changjiang River plume. Zhu et al. [62, 63] developed the first three-dimension, baroclinic, and terrain-following coordinate numerical model focusing on the Changjiang River plume. With this tool, they highlighted that (1) the increasing runoff does not necessarily result in enhanced northeastward plume extension; (2) the Taiwan warm current flows along the bathymetry, which does not interact with the Changjiang River Plume; (3) the circulation induced by the Yellow Sea Cold Water Mass (YSCWM) is important for the summertime Changjiang River plume extension; and (4) the southerly wind in summer favors the northeastward plume extension. The YSCWM is in the bottom layers of the central Yellow Sea, due to the seasonal variation of sea surface heat flux [19, 59]. The rapid warming in spring and summer produces a strong thermocline in the Yellow Sea, which reduces the vertical mixing and keeps the bottom water temperature lower than 8°C in summer season. However, the YSCWM is often located in the Yellow Sea Trough that is distant from the Changjiang River Estuary, and hence its role in regulating the Changjiang River plume is debatable. Also using a numerical model, Chang and Isobe [6] suggested that the wind and the “Taiwan-Tsushima Warm Current System” greatly controls the summertime plume extension.

Interestingly, it seems that these model results were inconsistent with the previous observational studies, which indicated that the observed Changjiang River plume could shift northeastward even without favorable winds (e.g., [23, 30, 60]). Moreover, the modeled Changjiang River plume often confusingly extended northward (NOT northeastward!) along the Jiangsu Coast, distinct from the observations. For example, in Chang and Isobe [6], the modeled Changjiang River plume even reached the northern tip of the Shandong Peninsula. The unreal northward plume extension is opposite to the Coriolis effect, which is often termed as “up-shelf intrusion.” Up-shelf plume intrusion occurs frequently in river plume intrusions [8, 9, 12, 16, 17, 22, 55], which was believed to be an artifact of numerical simulation. Many studies set an artificial down-shelf background current, solely to prevent the up-shelf intrusion (e.g., [9, 54]). Zhu et al. [62] set a strong southward-flowing Subei Coastal Current to prevent northward plume propagation. However, the existence of southward-flowing Subei Coastal Current in summer is highly debatable. Liu et al. [29] observed that under the southerly summer monsoon, the movement of Subei Coastal Water was actually northward. The Subei Coastal Current set in Zhu et al. [62] actually served as the background current. Some researchers thought that the modeled up-shelf plume intrusion is a realistic phenomenon

(e.g., [31]), and they raised the Changjiang River plume as an example. Unfortunately, they probably confused the observed northeastward offshore extension with the modeled northward up-shelf intrusion, which are substantially different.

One overlooked dynamic factor in these previous studies is the tide, which is very energetic in the Yellow and East China Sea. As indicated by the dominant tide constituent, M₂, the Changjiang River Estuary is influenced by two distinct tide systems: the progressive tide in the East China Sea and the rotating tide in the Yellow Sea (**Figure 3**). Tide wave from the Northwest Pacific propagates nearly parallel to the Ryukyu Islands, entering the East China

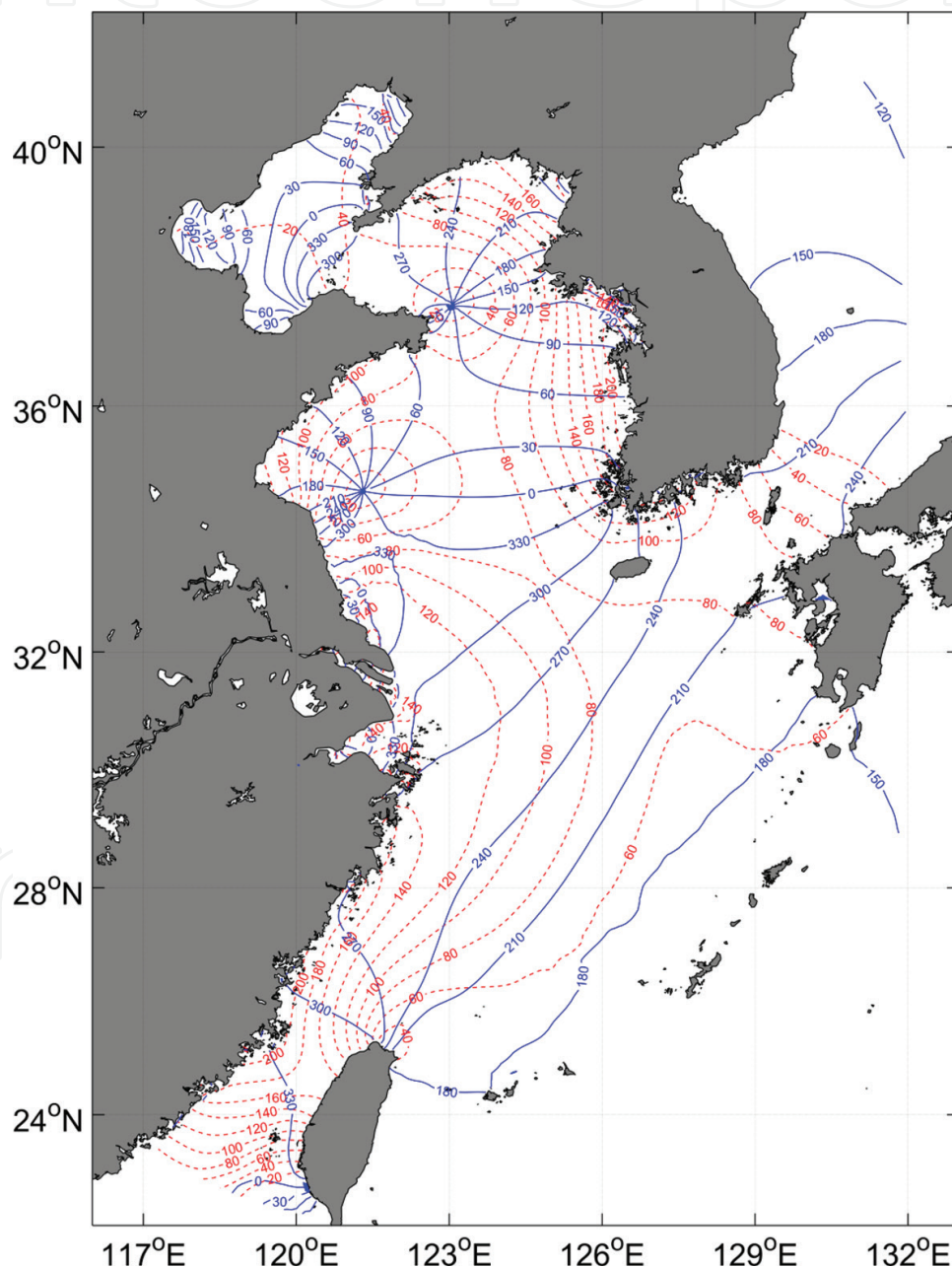


Figure 3. Co-tide map of the M₂ tide constituent. The blue solid lines are the co-phase lines with an interval of 30°, and the red dashed lines are the co-amplitude lines with an interval of 20 cm.

Sea and marching northwestward to the Changjiang Estuary. Off the river mouth, the co-phase lines become denser due to the shallowness of topography, which reduces the tidal wave speed. Annually averaged tidal range at the Changjiang River mouth is 2.67 m, and the maximum tidal range reaches 4.62 m. Gao et al. [14] highlighted the significant intra-tidal variability of the Changjiang River plume near the river mouth. Sampling at different tidal phases can result in a distinct salinity distribution. Moon et al. [34] found that the spring-neap variation of the tidal mixing can detach the diluted water from the Changjiang River plume at the slope region of the Changjiang Bank. Rong and Li [37] and Li and Rong [26] found that the tidal forcing intensifies the down-shelf transport of Changjiang diluted water, since the tidal forcing arrested the frontal instabilities, and therefore more buoyant water was moved to the down-shelf. Here in this chapter, we will show that the tidal forcing is actually responsible for many unexplained phenomena of the Changjiang River plume.

3. Numerical model

The numerical model used was developed by Wu et al. [49]. The hydrodynamic kernel of our model is the ECOM-si [5] with a robust HSMT-TVD advection scheme developed by Wu and Zhu [47] to solve the transport equations. The model used the modified Mellor and Yamada level 2.5 turbulent closure model [13, 32] for vertical mixing and τ scheme of Smagorinsky [40] for horizontal mixing. A wet/dry scheme was included with a minimum depth of 0.25 m. The model domain covered the entire East China Sea, Yellow Sea, Bohai Sea, and parts of the Pacific Ocean and the Japan Sea. The model grid mesh spanned 272×285 cell indices in the horizontal. Off the river mouth, the model mesh was about $2 \text{ km} \times 3 \text{ km}$ (in two directions). Twenty σ layers were used in the vertical with refined upper layer thicknesses. For a typical depth of 60 m off the Changjiang River mouth, the upper 10 m of the water column had eight layers. The open boundary was driven by the shelf currents and the tide currents. Surface heat flux was included in the model by the monthly data from NCEP (National Centers for Environmental Prediction). A bulk formula suggested by Ahsan and Blumberg [1] was used to calculate the atmospheric radiation (long-wave radiation), the evaporation heat flux, and the sensible heat flux.

4. Model validation

4.1. Validation of monthly mean salinity field

Model performance was evaluated with the monthly mean salinity documented by the Editorial Board for Marine Atlas [2]. In this numerical experiment, the model was driven with the climatological monthly runoff (based on historic observations by the Changjiang Water Resource Commission) and wind (from NCEP/CFSR) as well as 11 harmonic tidal current constituents. The model spun up for one year and the results of the second year were analyzed. The comparisons between the modeled monthly mean salinity and the Atlas' data in four selected months are shown in **Figure 4**. The modeled 30-psu isohalines (thick white lines)

were compared with those from the Editorial Board for Marine Atlas [2] (dashed red lines), which showed that the model performance were reliable.

4.2. Validation of cruising survey

The model was further validated with the in-situ data of surface salinity and temperature obtained in July 19–28, 2016. The model was driven by the daily runoff (observed by the Changjiang Water Resource Commission), 6-hourly wind, and 11 harmonic tidal current constituents.

Model results at the sampling locations and time of each observation were plotted for comparison (**Figure 5**). In the survey period, the Changjiang River plume featured a typical north-eastward summertime extension, covering a large area outside the river mouth (**Figure 5a**).

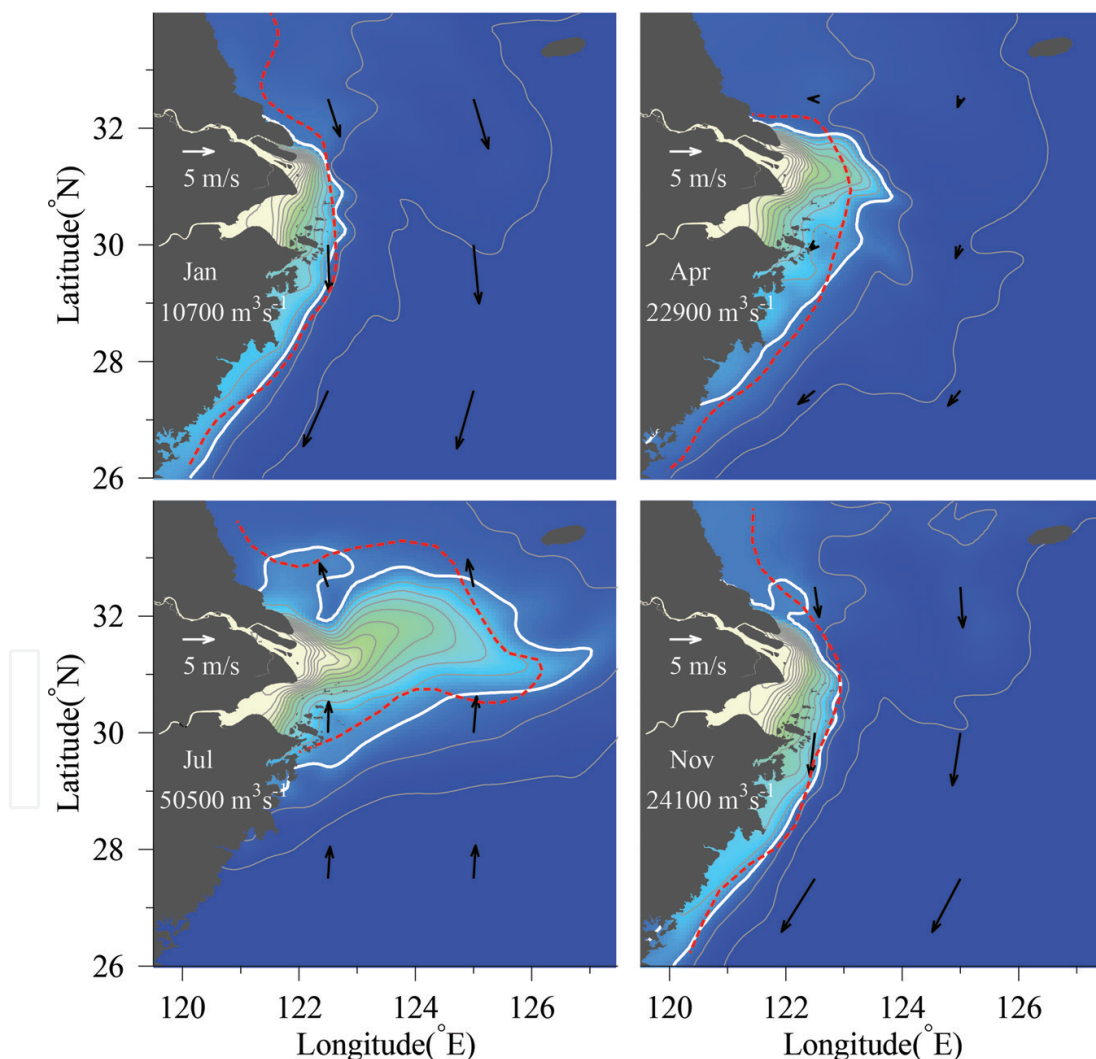


Figure 4. Sea surface salinity resulting from the climatological run in four selected months. The arrows are the monthly climatological wind. Monthly Changjiang River discharges are labeled. The contour interval of surface salinity is 2 psu, and the 30-psu contour is highlighted with thick white line. Dashed red line shows the 30-psu isohaline digitized from Editorial Board for Marine Atlas [2].

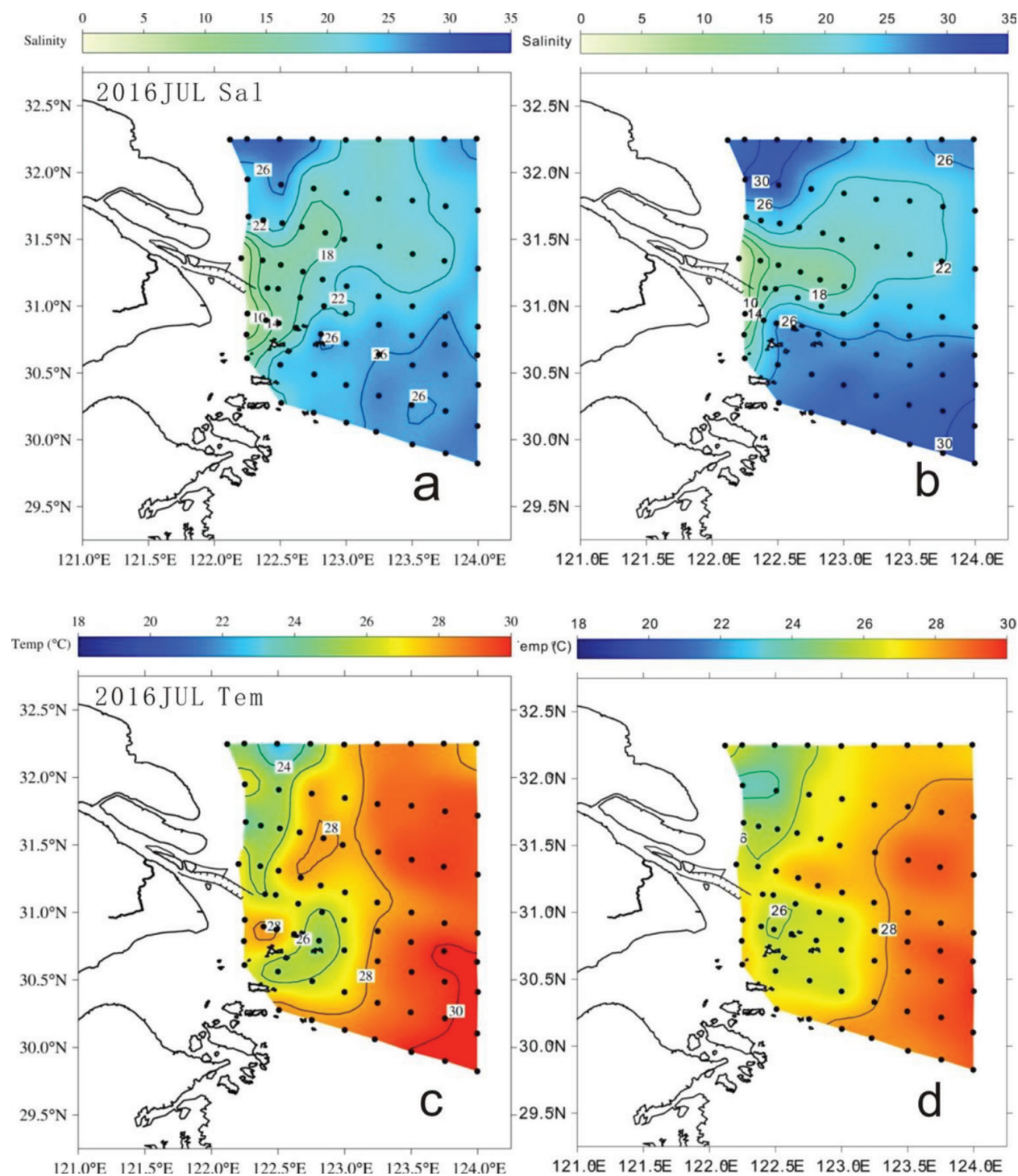


Figure 5. Comparisons between the observed ((a) and (c), dots signify the sampling stations) and the modeled ((b) and (d)) surface salinity ((a) and (b)), and temperature ((c) and (d)) distributions during July 2016.

Outside the river mouth, the sea surface temperature was generally high, but there were also some cold water patches near the river mouth, produced by strong tidal mixing that brings the bottom cold water to the sea surface. Overall, the model reproduced these features fairly well.

5. Suppression of up-shelf plume intrusion by tide

We used the validated numerical model to explore the tidal modulation mechanism on the Changjiang River plume [49]. Two numerical experiments were set up (Exp1 and Exp2). External forcings such as the wind and shelf currents were excluded for the moment, with only the runoff and tide retained.

5.1. Changjiang River plume without the tide

Previous nontidal simulations on the Changjiang river plume often gave an unreal massive up-shelf extension along the Jiangsu Coast (e.g., [6]). Our simulation (Exp1) reproduced this feature with tidal forcing excluded as previous studies. A large portion of the Changjiang diluted water spreads along the Jiangsu Coast after leaving the river mouth (**Figure 6A**), and the downstream current occurred only at the offshore edge of the plume. A train of wave was detected as well at the plume front, which was caused by baroclinic

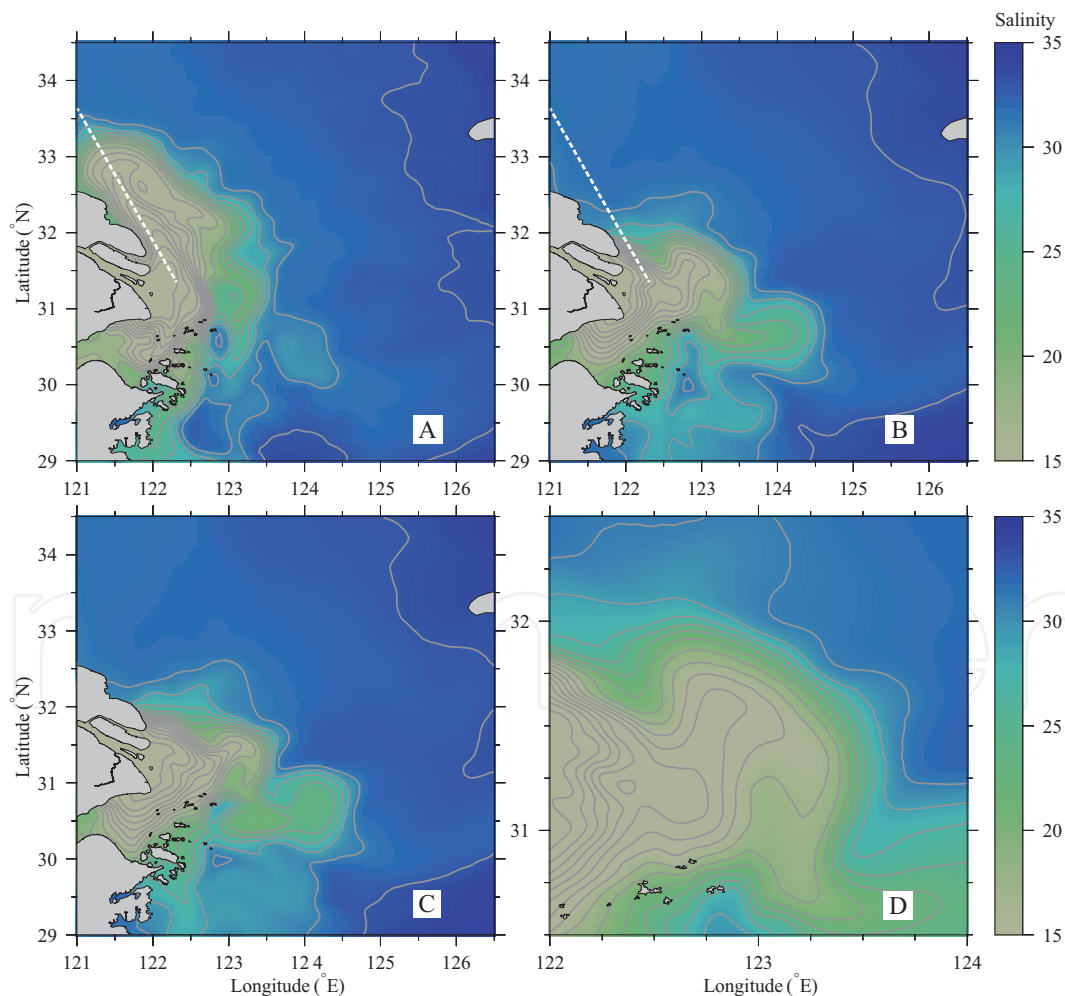


Figure 6. (A) Modeled surface salinity with river discharge only. (B) Tidal-averaged surface salinity during spring tide from the simulation with river discharge and tide. (C) Same as B but during the neap tide. (D) A zoom-in view of B.

instability [10]. Without the tidal forcing, the Changjiang River plume featured an expected anticyclonic bulge-like rotation [7, 54], but was elongated dramatically and extended to the upstream.

Similar up-shelf plume extension occurred frequently in previous numerical simulations for other realistic or idealized river plumes with settings similar to Exp1 (i.e., without tide, wind, nor ambient currents) [8, 9, 12, 16, 17, 22, 55]. Although many researchers believed that such an upstream plume extension is a model artifact, Matano and Palma [31] argued that such a characteristic is associated with the geostrophic adjustment the buoyant discharge, which creates an onshore baroclinic gradient force that drives a proportion of the discharge in the upstream direction. The plume extension from Exp1 is thus not surprising, and similar simulation results can be found in several other numerical studies of the Changjiang River plume in which the tide was excluded.

5.2. Influence of the tide in arresting the upstream extension

A common problem of Exp1 and previous simulations is the absence of tidal forcing. Massive up-shelf extension vanishes when the tidal forcing was added in Exp2 (**Figure 6B**). Instead of generating any downstream background current, the tide can produce an upstream residual current along the Jiangsu Coast due to its nonlinear interaction with the shallow topography, as is reported by Wu et al. [48]. Hence, it is not the down-shelf current that arrests the upstream extension of Changjiang River plume.

The actual mechanism is the tidal mixing. It is well known that the East China Sea and Yellow Sea have a meso- to macroscale tide system (**Figure 3**). Tidal range exceeds 4 m in spring tide around the Changjiang River Estuary. Moreover, the bathymetry is shallow around the river mouth. Hence, due to the strong tide and shallowness, tidal mixing is very strong around the Changjiang River Estuary. To address this point, we can look at the sectional profiles of salinity and turbulent viscosity along the Jiangsu Coastal with and without the tidal forcing (**Figure 7**). Without the tidal forcing, high stratification occurs near the surface (**Figure 7A**) since the turbulent viscosity was small (**Figure 7C**). With the tidal forcing included, the water column became well mixed (**Figure 7B**) since strong turbulent mixing occurred in the middle and lower layers (**Figure 7D**). A strong along-coastal baroclinic gradient was thereby formed at the northern side of the Changjiang River mouth, which drove a cross-coastal flow and prevented the upstream extension of the plume. It should be emphasized again that tidal mixing was not considered in previous model studies that produced the up-shelf plume extension. Because the tide exists at most regions of the world, this may give an additional explanation as to why most river plumes turn to the downstream direction besides the Coriolis forcing.

5.3. Tide-forced plume patterns

Besides arresting the upstream plume extension, the tidal forcing also modulated the Changjiang River plume in other remarkable ways. During the spring tide, the Changjiang River plume turned to the downstream at first inside the 30-m isobath, rotated

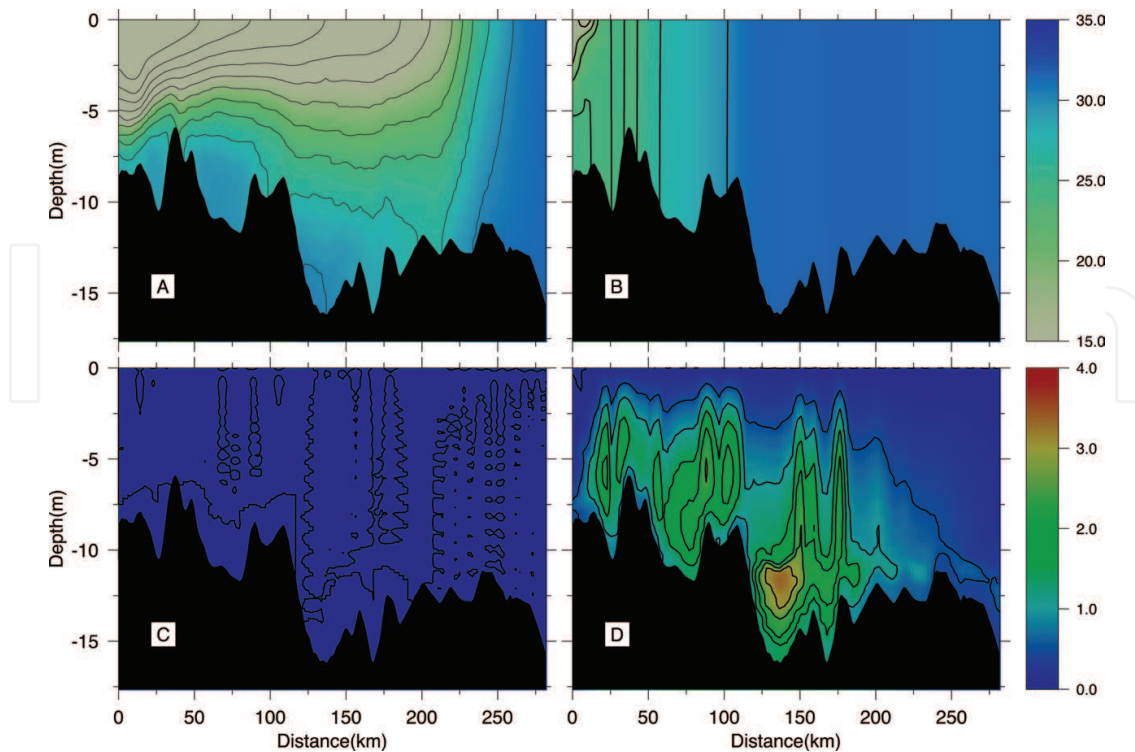


Figure 7. Sectional salinity (upper panels) and vertical turbulent viscosity (lower panels) (unit: $10^{-2} \text{ m}^2 \text{ s}^{-1}$) from Exp1 (left panels) and Exp2 (right panels). For section position, see **Figure 6**.

northeastward at approximate 122.5°E , and then rotated anti-cyclonically to the downstream (**Figure 6B**, a zoom-in view was shown in **Figure 6D**). A significant bulge occurred around the head of submarine canyon. However, such a bulge was weakened during the neap tide (**Figure 6C**), which implied that strength of the tide probably impacted on the bulge. The detail mechanisms responsible for this spring-neap variation of plume bulge are still unclear.

Interestingly, because of the rotation of the bulge, a northeastward freshwater tongue occurred near 122.5°E (during the spring tide, **Figure 6D**) or 123°E (during the neap tide, **Figure 6C**). Comparing with the nontidal simulation results, it seems that the tidal forcing is responsible for the northeastward turning of the Changjiang River plume, at least in the near field. Hence, it is understandable that why this turning can occur under various wind and runoff conditions, as was pointed out by previous studies.

5.4. Tidal modulation on river plume under the wind and shelf currents

Superimposing the southerly wind of 4 m s^{-1} and shelf currents, both model runs with (Exp3) and without tide (Exp4) showed a northeastward extension of the Changjiang River plume (**Figure 8**), but significant difference can also be found. Without tide, the plume also extended northward strongly due to the up-shelf plume intrusion (**Figure 8A**). Mao et al. [30] used the 26-psu isohaline as the exterior edge of the main body of Changjiang diluted water and the 32-psu isohaline as the extending edge of diluted water. Here, we use the 16-psu isohaline

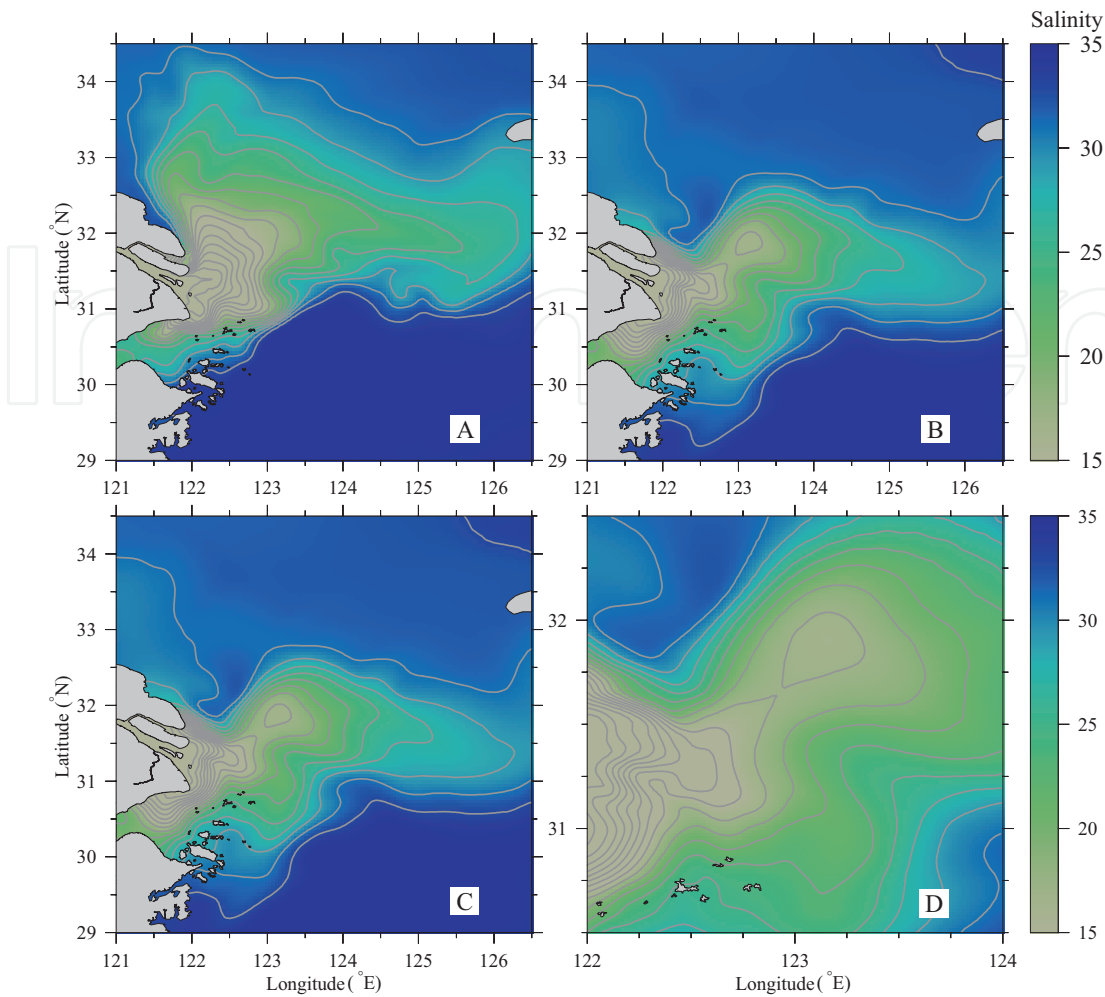


Figure 8. Surface salinity and current from Exp3 (A), tidal-averaged surface salinity during the spring tide (B) and the neap tide (C) from Exp4. (D) A zoom-in view of B.

additionally as the edge of freshwater. Defining A_s and V_s as the area and volume with salinity less than s (outside the Changjiang River mouth), respectively, the areas and volumes outside the 10-m isobath are shown in **Table 1**. A_{32} and V_{32} do not show significant differences with or without tide, while A_{26} and V_{26} are distinct. With the tidal forcing, the area and volume of the main body of diluted water are only about 60 and 70%, respectively, of the nontidal case. This is expected because the tide enhances vertical mixing and increases the surface salinity. Almost no differences can be found between spring and neap tides for A_{26} and V_{26} but significant differences appeared for those with salinity less than 16 psu. During spring tide, A_{16} and V_{16} were only 42 and 61%, respectively, of their values during neap tide. The biggest A_{16} but the smallest V_{16} under the nontidal case indicates that the plume was very thin without tide. These results also indicate that, in the near-field, the plume is highly varied during the spring-neap cycle, while, in the far field, it is less influenced.

South to the Changjiang River mouth, the ambient current is northward because of both the southerly wind and Taiwan warm current (**Figure 8**). Most of the Changjiang diluted

	S < 16		S < 26		S < 32	
	Area (km ²)	Volume (km ³)	Area (km ²)	Volume (km ³)	Area (km ²)	Volume (km ³)
Without tide	10,589	25	61,843	295	483,469	9428
Spring tide	4193	26	38,542	213	469,514	9903
Neap tide	9872	42	38,503	213	477,769	10,048

Table 1. Plume areas and volumes (with salinity less than 16, 26, and 32) during the spring and neap tides outside the isobath 10 m.

water spreads northeastward during both spring tide (**Figure 8A**) and neap tide (**Figure 8B**). During spring tide, the near-field plume is almost the same as that without external forcing (**Figure 6B**). The recirculating plume bulge vanished and joined into the far-field water because of the wind-induced mixing and the northeastward Ekman transport. The Changjiang River plume turned to the northeastward at 122.5°E (**Figure 8B**), almost the same place as the no-wind case (**Figure 6B**).

The minor southeastward branch of the Changjiang River plume can be identified during spring tide (**Figure 8B**). The bifurcation point was near the head of the submarine canyon. A strong southeastward residual current occurred on the slope, which was almost the same as that of Exp2 (**Figure 6B**), which resulted from tidal rectification. Such a residual current favors the diluted water flowing southward along the Zhejiang Coast. However, if we do not include the tide, the southward extended branch of the Changjiang River plume is greatly weakened, as is shown in **Figure 8A**.

5.5. Effect of wind direction

The wind field of the YECS region varies significantly both temporally and spatially. Therefore, the observed salinity distribution of the Changjiang River mouth was often distinct from the climatological situation. Here, we investigate how the Changjiang River plume is altered under different wind directions (i.e., the southeasterly wind (Exp5) and southwesterly wind (Exp6), respectively) with the same wind speed of 4 m s⁻¹.

Only the results during spring are shown (**Figure 9**). A major difference occurs in the far-field plume regions. A southeast wind results in a northeast Ekman transport, and therefore in the far field, the northeastward plume branch was better developed and was toward the Jeju Island. The southeastward plume branch that bifurcated at the head of the canyon had almost vanished. The southwest wind produced a southeast Ekman pumping, resulting in a south-eastward extension of the Changjiang River plume in the far field. The southeastward plume branch was more evident than the case of south or southeast wind, but the northeastward plume branch was less evident. Nevertheless, in the near field, the plume pattern remained the same under all wind directions, even under the no-wind condition. This indicated that the tidal modulation is an essential mechanism in shifting the Changjiang River plume to the northeastward in summer.

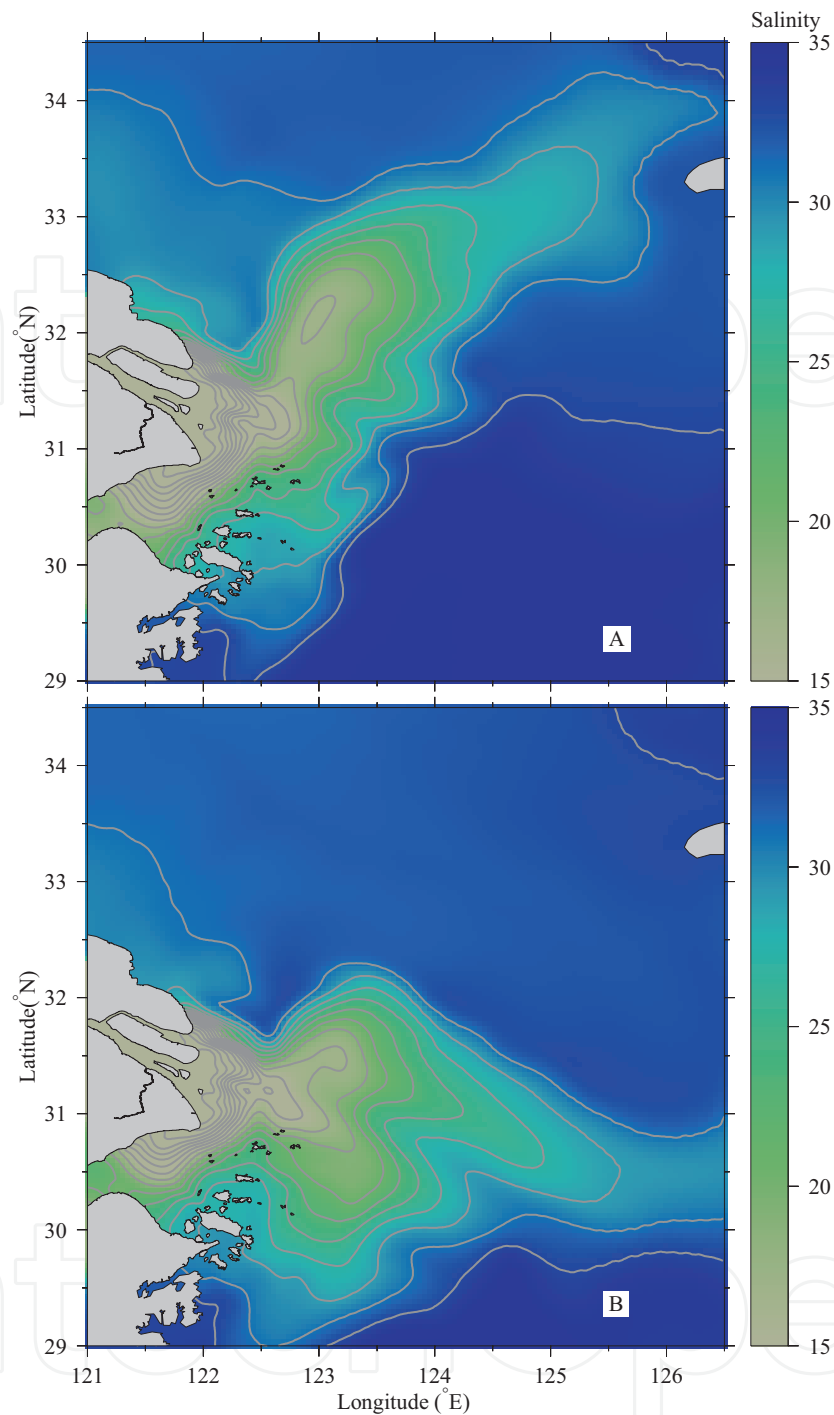


Figure 9. Tidally averaged surface salinity during spring tide under (A) southeasterly wind (i.e., Exp5) and (B) southwesterly wind (i.e., Exp6).

6. Characteristics of the Changjiang River plume under realistic forcings

In climatological model results, the Changjiang River plume spreads to the south along the Zhejiang Coast in winter, whereas turns to the northeast and can even reach the Jeju Island

in summer. It is important to know whether these plume patterns obtained via climatological run are still significant in the realistic environment. Therefore, we conducted a long-term (2000–2008) realistic simulation of the Changjiang River plume and analyzed the modeled surface salinity with empirical orthogonal function (EOF) [50]. The modeled hourly SSSs from year 2001 to 2008 were output and interpolated to a $0.25^\circ \times 0.25^\circ$ mesh to save the computational cost. The SSS time series at each grid point was low-pass filtered with a cutoff window of 34 h to remove the tidal signals, and the filtered salinity field on each day was analyzed with the EOF method.

Three leading EOF modes are shown in **Figure 10**, which contributed 42.9, 14.6, and 9.5%, respectively, of a total of 67%, for the total variance. Mode 1 (**Figure 10A** and **B**) shows the

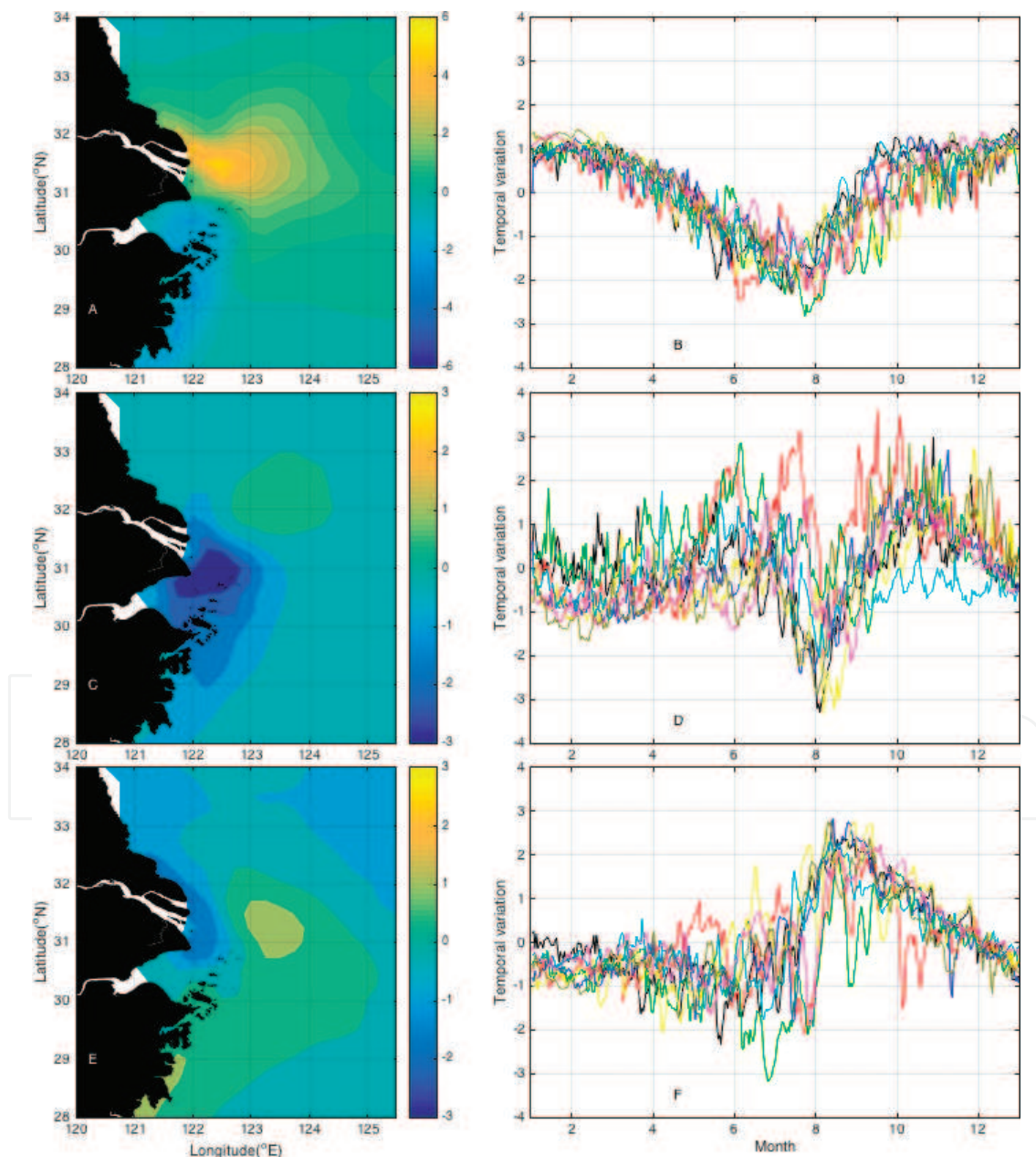


Figure 10. Three leading EOFs (A, C, and E) of the surface salinity anomaly and their PCs (B, D, and F).

two major branches of the Changjiang River plume. From May to August, there is a negative salinity anomaly located northeast to the river mouth. In the remaining months, the negative salinity anomaly is located along the Zhejiang Coast. This remarkable seasonal variation is consistent with the northeastward and southward plume branches. Mode 2 (**Figure 10C and D**) shows that the plume salinity is periodically increased near the river mouth but decreased northeast to the river mouth. The latter one has been recognized as the plume detachment in recent years based on a series of observational studies (e.g., [27]) and modeling studies [34, 37, 39, 49, 52]. Mode 3 (**Figure 10E and F**) suggests that there is a negative salinity anomaly located along the Jiangsu Coast mostly in summer and autumn seasons, corresponding to the northward plume extension.

By analyzing the PCs of EOF (**Figure 10B, D and F**), we can understand the variations of EOF modes at different time scales. We separated the time scales as short (<20 days) and long (>20 days) based on the spectrum analysis. The long-term scale represents the seasonal variations, while the short-term scale represents the variations due to tide and weather events. In this way, we found that the Mode 1, that is, the alternation between propagating northeastward and southward, is mainly controlled by runoff and wind at seasonal time scales. It is also significantly modulated by tide and synoptic wind events. Mode 2, that is, the plume detachment and salinity change near the river mouth, is mainly correlated to the tidal range. This confirmed the previous study that the plume detachment northeast of the Changjiang River is mainly caused by the intense tidal mixing in spring tide [34, 49]. Mode 3, that is, part of the Changjiang River plume extending along the Jiangsu Coast, is mainly correlated to the tidal range but insensitive to the river discharge and wind.

Overall, from the EOF analysis, it can be seen that the Changjiang River plume mainly extends in three pathways, that is, the northeastward, southward, and northward branches. The former two branches are accounted for by Mode 1, which represents the dominant seasonal variation of the Changjiang River plume. The northeastward plume branch dominates during the flood season when the Changjiang discharge is huge and the wind is southerly. During the dry season with reduced discharge and enhanced northerly wind, the southward branch is developed, and the northeastward one vanishes. The northward plume branch along the Jiangsu Coast is a new finding, which occurs mostly in summer and autumn seasons.

7. Extension of Changjiang River plume to the Jiangsu Coast

The above analysis indicates that a small portion of the Changjiang River plume extends to the Jiangsu Coast, even in autumn when the wind turns northerly. Such an extension is in a direction opposite to that of the coastally trapped wave (i.e., the upstream direction). Unlike the massive up-shelf intrusion simulated by nontidal plume models (**Figure 6A**), this plume branch is weak. Such a weak plume extension diluted the seawater in the Subei Coastal Water, producing the so-called Subei low salinity water, which has been observed by numerous surveys (e.g., [33, 46, 61]) and is shown in climatological data ([2, 41]).

7.1. Freshwater flux into the Subei Coastal Water

To explore the dynamics that transports the Changjiang River plume to the Subei Coastal Water, we applied the flux decomposing method along a section SEC crossing this plume branch at 32.5°N. Considering the freshwater “concentration” $f = (s_o - s)/s_o$, the freshwater transport at a unit width of water column over a tidal cycle is defined as:

$$T = \left\langle \int_{-H}^0 v f dz \right\rangle \quad (1)$$

where v is the velocity component normal to the section (i.e., northward component); $\langle \rangle$ is a low-pass filter operator (with a cutoff window of 34 h). Decompose the freshwater concentration f into:

$$f = \langle \bar{f} \rangle + \bar{f}' + f' \quad (2)$$

where \bar{f} is the depth averaged freshwater concentration, $\bar{f}' = \bar{f} - \langle \bar{f} \rangle$ is the tidal oscillatory term of the depth averaged freshwater concentration, and $f' = f - \bar{f}$ is the vertical deviation of the freshwater concentration. v is treated in the same way. For the water depth, $H = \langle H \rangle + H'$. Therefore,

$$\begin{aligned} T &= \langle H \rangle \langle \bar{v} \rangle \langle \bar{f} \rangle + \langle H' \bar{v} \rangle \langle \bar{f} \rangle + \langle H' \bar{f}' \rangle \langle \bar{v} \rangle + \langle H \bar{v}' \bar{f}' \rangle + \langle H \bar{v}' \bar{f}' \rangle \\ &= T_1 + T_2 + T_3 + T_4 + T_5 \end{aligned} \quad (3)$$

in which T_1 is the Eulerian transport that is related to mean flow. T_2 is the Stokes transport that results from the nonlinear interaction between the sea surface tidal fluctuation and the tidal current. T_1 and T_2 represent the transport due to sub-tidal water mass transport. T_3 is almost zero in this study, and the sum of T_3 and T_4 is the tidal pumping transport that results from the tidal asymmetry among the freshwater concentration, water depth, and velocity. T_5 is the shear transport due to the vertically sheared structure of the concentration and velocity. T and T_1 through T_5 were integrated along SEC, respectively.

The freshwater transport across SEC is northward from March to November (**Figure 11**), although the northward plume branch mainly appears from July to October, possibly because of the inaccurate ambient ocean salinity (34 psu) in this region. Nevertheless, it means that the northward water mass transport persists along the Jiangsu Coast. The northward freshwater transport is mainly contributed by the Stokes transport and is enhanced in summer but weakened in winter by the Eulerian transport. The shear transport and tidal pumping transport were generally small.

As the Stokes transport dominates the northward freshwater transport along the Jiangsu Coast, even in the months with the northerly wind, the northward plume can develop. Under the persistent northward Stokes transport, once the Changjiang discharge rises and thereby increases the $\langle f \rangle$, or the wind causes the Eulerian transport to also be northward, the northward plume branch develops.

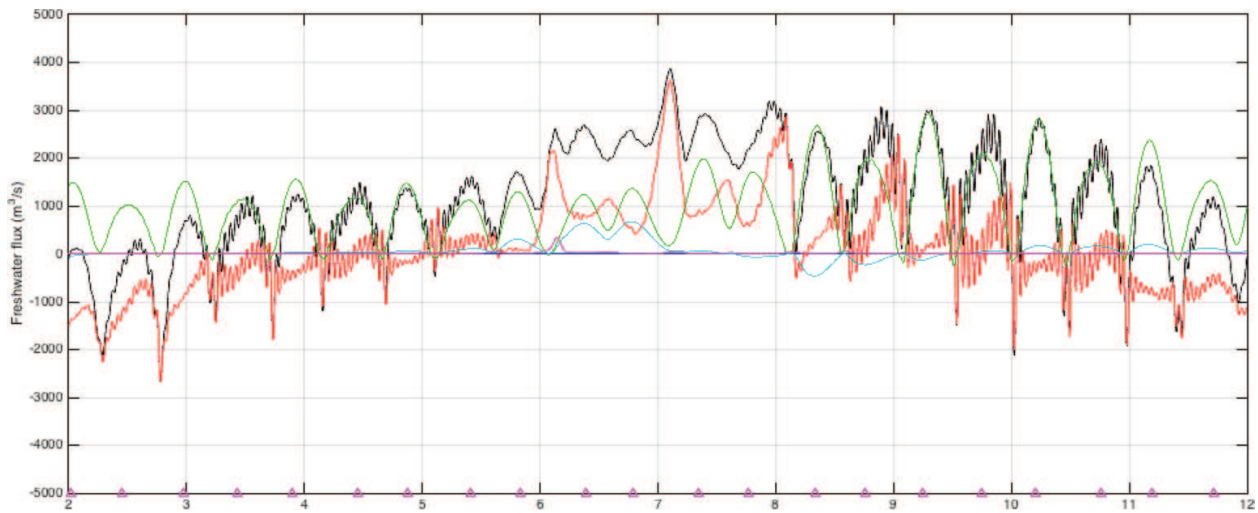


Figure 11. Freshwater flux and their decomposed components across the northward plume branch, with positive values to the north. Triangles at the bottom signify the times of the spring tides. Black line: total freshwater flux (T). Red line: Eulerian transport (T1). Green line: Stokes transport (T2). Blue line: T3. Light blue line: T4. Purple line: stress transport (T5).

7.2. Residual currents in response to wind and tide

Since the transport of the northward plume branch is determined by the sub-tidal water mass transport, we can understand its dynamics by investigating the residual currents around the Jiangsu coastal waters. Tide and wind are two most energetic forcings in the Jiangsu coastal waters. In fact, tide-induced residual currents are general in coastal regions [20, 24, 43], with their direction consistent to the projection of the major flood vector on the coast [56]. Two diagnostic numerical experiments were set, both of which only included the tide and 5 m s^{-1} wind forcing, with directions of southerly and northerly, respectively, representing the summer and autumn seasons.

Eulerian and Stokes transports of the Changjiang diluted water in Eq. (3) is determined by the residual water mass transport, which can be decomposed into:

$$\left\langle \int_{-H}^0 \vec{v} dz \right\rangle = \langle H \vec{v} \rangle = \langle H \rangle \langle \vec{v} \rangle + \langle H' \vec{v}' \rangle \quad (4)$$

by using the same method as Eq. (2). Normalized by tidally averaged depth, one can get:

$$\vec{V}_L = \vec{V}_E + \vec{V}_S \quad (5)$$

where

$$\vec{V}_L = \langle \int_{-H}^0 \vec{v} dz \rangle / \langle H \rangle, \vec{V}_E = \langle \vec{v} \rangle, \vec{V}_S = \langle H' \vec{v}' \rangle / \langle H \rangle \quad (6)$$

\vec{V}_E is the traditional depth averaged Eulerian residual current; \vec{V}_S is noted as the mass transport Stokes drift [18, 43]; and their sum \vec{V}_L is the residual transport velocity. As the contributions of tidal pumping and shear transport are negligible for the northward plume branch, \vec{V}_E , \vec{V}_S , and \vec{V}_L can represent the transport of diluted water.

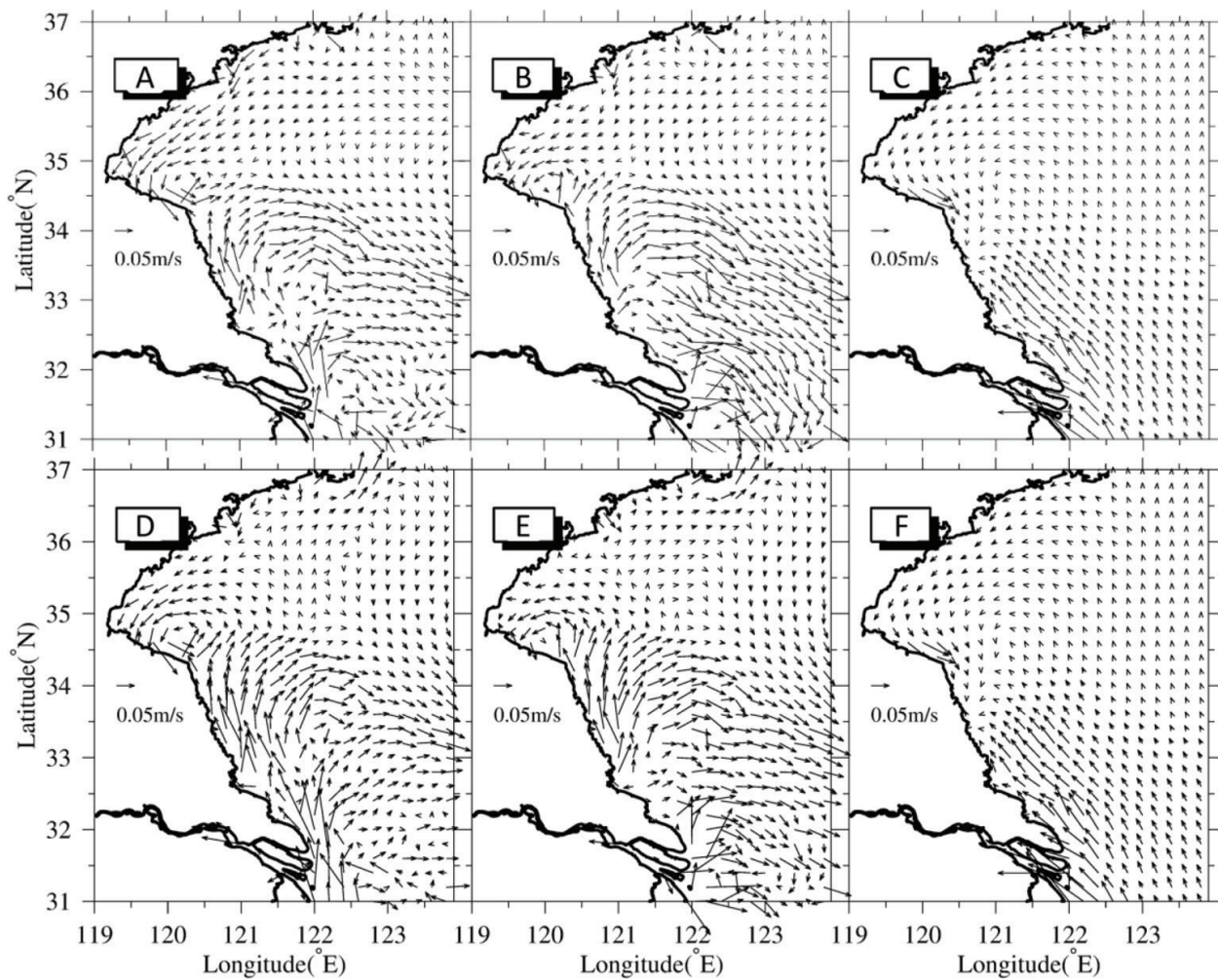


Figure 12. Residual transport velocity (A and D) and its decompositions of the Eulerian residual current (B and E) and the Stokes drift (C and F) during the spring tide. A, B, and C are the results under the 5 m s^{-1} northerly wind; D, E, and F are the results under the 5 m s^{-1} southerly wind.

Strong nonlinear interaction between wind and tide can be found from **Figures 12 and 13**. During the neap tide, \vec{v}_L is controlled by the Eulerian residual current, while the Stokes drift is negligible since the tidal range is small. The Eulerian residual current is northward when the wind is southerly but reverses when the wind turns to northerly. During the spring tide, however, the wind-driven circulation seems to be dampened significantly, and the residual current patterns are nearly under different wind directions. Although \vec{v}_L reverses its direction during neap tide as the wind direction changes, during the spring tide, it is basically northward from the Changjiang River mouth to $\sim 34^\circ\text{N}$ along the Jiangsu Coast.

From **Figures 12 and 13**, it can be seen that the Stokes drift essentially drives the up-shelf transport in the Subei Coastal Water, thus the extension of Changjiang River plume in this area. The formation mechanism of tide-induced Stokes drift is the nonlinear interaction between tidal elevation and tidal current, which is determined by tide tidal wave regime in the East China Sea and Yellow Sea [50]. Stokes transport is stable under various wind directions. This explains why the northward plume branch can exist not only during summer when the wind is southerly, but also can maintain itself in autumn when the wind has already turned to northerly.

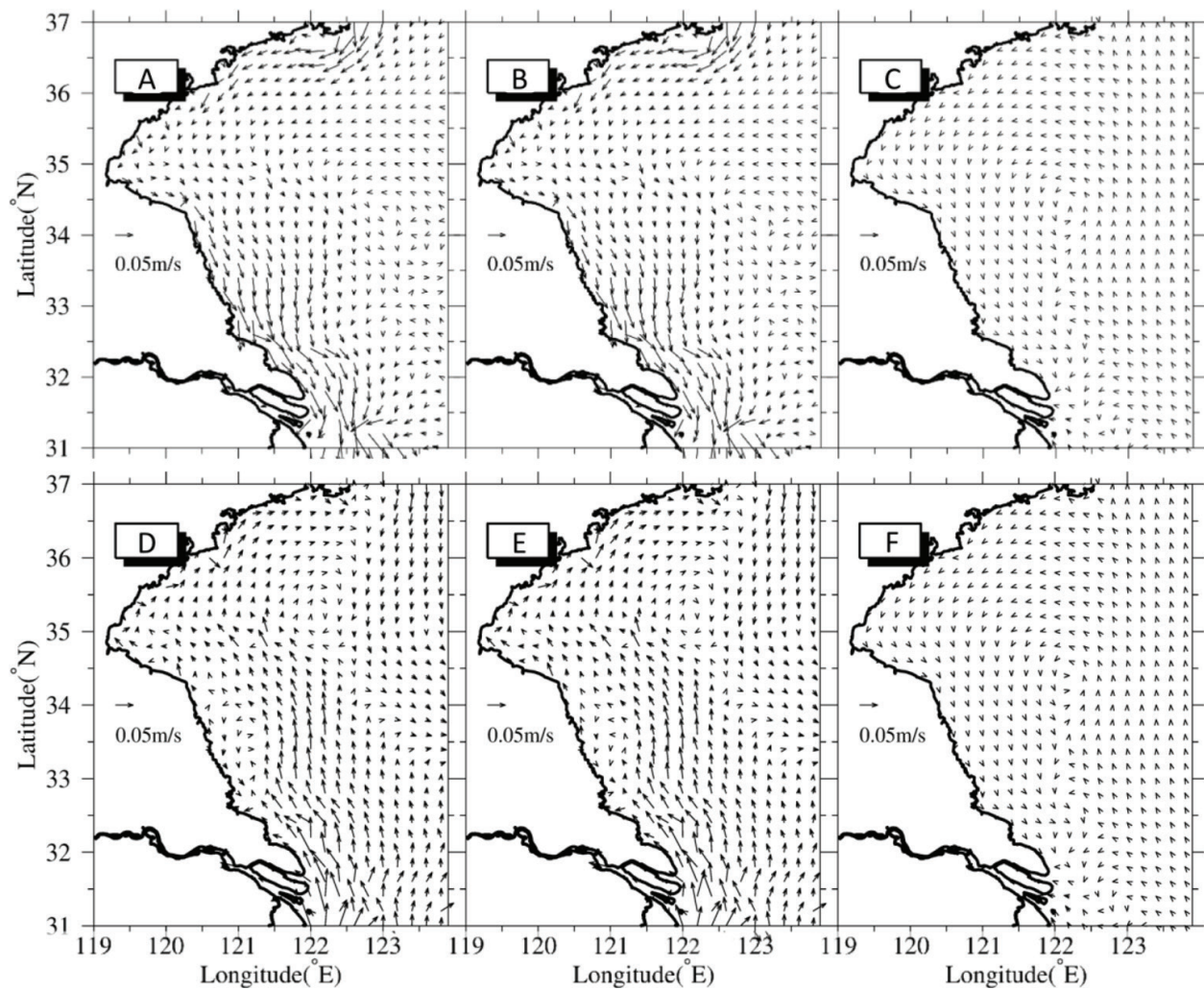


Figure 13. Same as Figure 12, except during the neap tide.

8. Conclusion

Researchers have worked on the Changjiang River plume for more than 60 years, which substantially promoted the understandings on the dynamics and environments in the Yellow and East China Sea. Looking back at the history, the academic studies on Changjiang River plume began very early in 1960s, when the basic characteristics were revealed. The research was interrupted by the Cultural Revolution in 1970s, and then resurged in 1980s and 1990s with numerous fantastic theoretical studies that attempted to reveal the dynamic mechanisms. No consensus, however, was reached during that period. In 1990s and 2010s, numerical simulation became a major method to study the Changjiang River plume, but the study was less active than those in 1980s and 1990s. One reason was that many physical oceanographers in China changed their research focus to the open ocean. Another reason, perhaps more importantly, is that the modeled river plume was often distinct from reality, which made the numerical models doubtful.

Since 2010, the tidal effect was found to be of essential importance in determining the characteristics of the Changjiang River plume. Moon et al. [34] and Rong and Li [37] found that it is

the tide that generates the massive plume detachment at specific locations. Li and Rong [26] found that it is the tide that remarkably strengthens the down-shelf transport of Changjiang River plume. Wu et al. [49] found that it is the tide that prevents the up-shelf plume intrusion, shifts the Changjiang River plume to the northeast outside the river mouth, and bifurcates the plume at the head of submarine canyon. Wu et al. [50] found that it is the tide that transports part of the Changjiang River plume to the Subei Coastal Water. Recently, Wu [51] further found that it is the tide that generates the cross-shelf penetration of Changjiang River plume in the Zhejiang-Fujian coastal water.

It is not to say that tide is the only important factor controlling the dynamics of the Changjiang River plume. Winds, shelf currents, and the river discharge itself are of course important in determining the dynamics around the Changjiang River Estuary. But the tidal effects were often overlooked before 2010, although it is no doubting that the tide is the most energetic movements around the Changjiang River Estuary. The reason could be that the tidal effect is highly nonlinear, and hence an elegant theory on dynamics can hardly be established. Most early studies just ignored the tidal forcing in theoretical or numerical studies. The existent classic plume theories, such as Yankovsky and Chapman [54] and Chapman and Lentz [9], were developed without considering the tidal effects. A question arises that on what degree these theories can be applied in and tidal area. Yellow and East China Seas is a perfect place to study the river plume, since this area is coinfluenced by massive river discharge, strong tide, energetic shelf circulation, and a typical seasonal monsoon. Many have been done, more await to be explored.

Acknowledgements

We appreciate Prof. Xiangshan Liang for his kind invitation for us to write this chapter. Some materials of this chapter have been previously published in journal articles, and the authors want to appreciate the previous reviewers and editors once again for their insightful comments and suggestions. This work was supported by National Natural Science Foundation of China (Grant no. 40806034) and the National Basic Research Program of China (2011CB409801).

Author details

Hui Wu^{1*}, Tianning Wu¹, Jian Shen² and Jianrong Zhu¹

*Address all correspondence to: hwu@sklec.ecnu.edu.cn

1 State Key Laboratory of Estuarine and Coastal Research, East China Normal University, Shanghai, P.R. China

2 Virginia Institute of Marine Science, College of William and Mary, Gloucester Point, Virginia, USA

References

- [1] Ahsan AQ, Blumberg AF. Three-dimensional hydrothermal model of Onondaga Lake, New York. *Journal of Hydraulic Engineering*. 1999;**125**(9):912-923
- [2] Editorial Board for Marine Atlas. *Ocean Atlas in Huanghai Sea and East China Sea (Hydrology)*. Beijing: China Ocean Press; 1992
- [3] Bai XZ, Wang F. Numerical study on the mechanism of the expansion of the Changjiang River diluted water in summer. *Oceanologia et Limnologia Sinica*. 2003;**34**(6):593-603
- [4] Beardsley R. Structure of the Changjiang river plume in the East China Sea during June 1980. In: *Paper Presented at Proceedings of International Symposium on Sedimentation on the Continental Shelf, with Special Reference to the East China Sea*. China Ocean Press; 1983
- [5] Blumberg A. A primer for ECOM-si, Technical report of HydroQual, 66. 1994
- [6] Chang PH, Isobe A. A numerical study on the Changjiang diluted water in the Yellow and East China Seas. *Journal of Geophysical Research: Oceans*. 2003;**108**(C9):3299
- [7] Chao S-Y. River-forced estuarine plumes. *Journal of Physical Oceanography*. 1988;**18**(1):72-88
- [8] Chao S-Y, Boicourt WC. Onset of estuarine plumes. *Journal of Physical Oceanography*. 1986;**16**(12):2137-2149
- [9] Chapman DC, Lentz SJ. Trapping of a coastal density front by the bottom boundary layer. *Journal of Physical Oceanography*. 1994;**24**(7):1464-1479
- [10] Chen C, Xue P, Ding P, Beardsley RC, Xu Q, Mao X, et al. Physical mechanisms for the offshore detachment of the Changjiang diluted water in the East China Sea. *Journal of Geophysical Research: Oceans*. 2008;**113**(C2):C02002
- [11] Dong L, Guan W, Chen Q, Li X, Liu X, Zeng X. Sediment transport in the Yellow Sea and East China Sea. *Estuarine, Coastal and Shelf Science*. 2011;**93**(3):248-258
- [12] Fong DA. *Dynamics of Freshwater Plumes: Observations and Numerical Modeling of the Wind-Forced Response and Alongshore Freshwater Transport*. Massachusetts Institute of Technology and Woods Hole Oceanographic Institution; Ph.D. thesis; Woods Hole; 1998
- [13] Galperin B, Kantha L, Hassid S, Rosati A. A quasi-equilibrium turbulent energy model for geophysical flows. *Journal of the Atmospheric Sciences*. 1988;**45**(1):55-62
- [14] Gao L, Li D-J, Ding P-X. Quasi-simultaneous observation of currents, salinity and nutrients in the Changjiang (Yangtze River) plume on the tidal timescale. *Journal of Marine Systems*. 2009;**75**(1):265-279
- [15] Gao S, Collins M. Holocene sedimentary systems on continental shelves. *Marine Geology*. 2014;**352**:268-294

- [16] Garvine RW. Penetration of buoyant coastal discharge onto the continental shelf: A numerical model experiment. *Journal of Physical Oceanography*. 1999;**29**(8):1892-1909
- [17] Garvine RW. The impact of model configuration in studies of buoyant coastal discharge. *Journal of Marine Research*. 2001;**59**(2):193-225
- [18] Hunter J. An investigation into the circulation of the Irish Sea. Oceanography Report 72-1. Menai Bridge, UK: Marine Science Laboratories, University College of North Wales; 1972
- [19] Hur H, Jacobs G, Teague W. Monthly variations of water masses in the Yellow and East China Seas, November 6, 1998. *Journal of Oceanography*. 1999;**55**(2):171-184
- [20] Ianniello J. Tidally induced residual currents in estuaries with constant breadth and depth. *Journal of Marine Research*. 1977;**35**:755-786
- [21] Isobe A, Ando M, Watanabe T, Senjyu T, Sugihara S, Manda A. Freshwater and temperature transports through the Tsushima-Korea Straits. *Journal of Geophysical Research: Oceans*. 2002;**107**(C7):3065
- [22] Kourafalou VH, Oey LY, Wang JD, Lee TN. The fate of river discharge on the continental shelf: 1. Modeling the river plume and the inner shelf coastal current. *Journal of Geophysical Research: Oceans*. 1996;**101**(C2):3415-3434
- [23] Le K-T. A preliminary study of the path of the Changjiang diluted water. *Oceanologia et Limnologia Sinica*. 1984;**15**(2):157-167
- [24] Li C, O'Donnell J. Tidally driven residual circulation in shallow estuaries with lateral depth variation. *Journal of Geophysical Research: Oceans*. 1997;**102**(C13):27915-27929
- [25] Li D, Zhang J, Huang D, Wu Y, Liang J. Oxygen depletion off the Changjiang (Yangtze River) estuary. *Science in China Series D: Earth Sciences*. 2002;**45**(12):1137-1146
- [26] Li M, Rong Z. Effects of tides on freshwater and volume transports in the Changjiang River plume. *Journal of Geophysical Research: Oceans*. 2012;**117**(C6):C06027
- [27] Lie HJ, Cho CH, Lee JH, Lee S. Structure and eastward extension of the Changjiang River plume in the East China Sea. *Journal of Geophysical Research: Oceans*. 2003;**108**(C3):3077
- [28] Liu Z, Xia D. A preliminary study of tidal current ridges. *Chinese Journal of Oceanology and Limnology*. 1985;**3**(1):118-133
- [29] Liu Z, Hu D. Preliminary study on the Huanghai Sea coastal current and its relationship with local wind in summer. *Acta Oceanologica Sinica*. 2009;**31**(2):1-7
- [30] Mao H, Gan Z-J, Lan S-F. A preliminary study of the Yangtze diluted water and its mixing processes. *Oceanologia et Limnologia Sinica*. 1963;**5**(3):183-206
- [31] Matano RP, Palma ED. The upstream spreading of bottom-trapped plumes. *Journal of Physical Oceanography*. 2010;**40**(7):1631-1650
- [32] Mellor GL, Yamada T. Development of a turbulence closure model for geophysical fluid problems. *Reviews of Geophysics*. 1982;**20**(4):851-875

- [33] Mi T-Z, Yao Q-Z, Meng J, Zhang X-L, Liu S-M. Distributions of nutrients in the southern Yellow Sea and East China Sea in spring and summer 2011. *Oceanologia et Limnologia Sinica*. 2012;**43**:678-688
- [34] Moon J-H, Hirose N, Yoon J-H, Pang I-C. Offshore detachment process of the low-salinity water around Changjiang Bank in the East China Sea. *Journal of Physical Oceanography*. 2010;**40**(5):1035-1053
- [35] Pan Y, Wang K, Huang S. Analysis on the path of transportation and diffusion of Changjiang diluted water. *Donghai Marine Science*. 1997;**15**(2):25-34
- [36] Pu Y, Xu X. The expansion of diluted water in the Changjiang (Yangtze R.) as seen from the variations in the runoff, water level and salinity. *Marine Science Bulletin*. 1983;**2**(3):1-7
- [37] Rong Z, Li M. Tidal effects on the bulge region of Changjiang River plume. *Estuarine, Coastal and Shelf Science*. 2012;**97**:149-160
- [38] Shen H. *Material Flux of the Changjiang Estuary*. Beijing: China Ocean Press; 2001
- [39] Shi JZ, Lu L-F. A short note on the dispersion, mixing, stratification and circulation within the plume of the partially-mixed Changjiang River Estuary, China. *Journal of Hydro-Environment Research*. 2011;**5**(2):111-126
- [40] Smagorinsky J. General circulation experiments with the primitive equations: I. The basic experiment. *Monthly Weather Review*. 1963;**91**(3):99-164
- [41] Su J, Yuan Y. *Oceanography of China Seas*. Beijing: China Ocean Press; 2005
- [42] Tang D, Di B, Wei G, Ni I-H, Wang S. Spatial, seasonal and species variations of harmful algal blooms in the South Yellow Sea and East China Sea. *Hydrobiologia*. 2006;**568**(1): 245-253
- [43] Tee K-T. Tide-induced residual currents, a 2-D nonlinear tidal model. *Journal of Marine Research*. 1976;**34**:603-628
- [44] Tong Y, Zhao Y, Zhen G, Chi J, Liu X, Lu Y, et al. Nutrient loads flowing into coastal waters from the main rivers of China (2006-2012). *Scientific Reports*. 2015;**5**:16678
- [45] Wang B, Xie L, Sun X. Water quality in marginal seas off China in the last two decades. *International Journal of Oceanography*. 2011;**2011**:731828
- [46] Wei Q, Zang J, Wei X, Liu L. The distribution of nutrients and the relationship of them with the circulation condition in the western southern Huanghai Sea in autumn. *Acta Oceanologica Sinica*. 2011;**33**(1):74-82
- [47] Wu H, Zhu J. Advection scheme with 3rd high-order spatial interpolation at the middle temporal level and its application to saltwater intrusion in the Changjiang Estuary. *Ocean Modelling*. 2010;**33**(1):33-51
- [48] Wu H, Zhu J, Choi BH. Links between saltwater intrusion and subtidal circulation in the Changjiang Estuary: A model-guided study. *Continental Shelf Research*. 2010;**30**(17): 1891-1905

- [49] Wu H, Zhu J, Shen J, Wang H. Tidal modulation on the Changjiang River plume in summer. *Journal of Geophysical Research: Oceans*. 2011;**116**(C8):C08017
- [50] Wu H, Shen J, Zhu J, Zhang J, Li L. Characteristics of the Changjiang plume and its extension along the Jiangsu Coast. *Continental Shelf Research*. 2014;**76**:108-123
- [51] Wu H. Cross-shelf penetrating fronts: A response of buoyant coastal water to ambient pycnocline undulation. *Journal of Geophysical Research: Oceans*. 2015;**120**(7):5101-5119
- [52] Xuan JL, Huang D, Zhou F, Zhu XH, Fan X. The role of wind on the detachment of low salinity water in the Changjiang Estuary in summer. *Journal of Geophysical Research: Oceans*. 2012;**117**(C10):C10004
- [53] Yang SL, Milliman JD, Xu KH, Deng B, Zhang X, Luo X. Downstream sedimentary and geomorphic impacts of the Three Gorges Dam on the Yangtze River. *Earth-Science Reviews*. 2014;**138**:469-486
- [54] Yankovsky AE, Chapman DC. A simple theory for the fate of buoyant coastal discharges. *Journal of Physical Oceanography*. 1997;**27**(7):1386-1401
- [55] Yankovsky AE. The cyclonic turning and propagation of buoyant coastal discharge along the shelf. *Journal of Marine Research*. 2000;**58**(4):585-607
- [56] Ye J, Garvine RW. A model study of estuary and shelf tidally driven circulation. *Continental Shelf Research*. 1998;**18**(10):1125-1155
- [57] Yu K. Two dimensional numerical calculation of residual current and salinity at the Changjiang River Estuary. *Oceanologia et Limnologia Sinica*. 1990;**21**(1):92-96
- [58] Yuan D, Zhu J, Li C, Hu D. Cross-shelf circulation in the Yellow and East China Seas indicated by MODIS satellite observations. *Journal of Marine Systems*. 2008;**70**(1):134-149
- [59] Zhang S, Wang Q, Lü Y, Cui H, Yuan Y. Observation of the seasonal evolution of the Yellow Sea Cold Water Mass in 1996-1998. *Continental Shelf Research*. 2008;**28**(3):442-457
- [60] Zhao B. On the extension of Changjiang diluted water. *Acta Oceanologica Sinica*. 1991;**13**(5):600-610
- [61] Zhou F, Su J, Huang D. Study on the intrusion of coastal low salinity water in the west of southern Huanghai Sea during spring and summer. *Acta Oceanologica Sinica (in Chinese)*. 2004;**26**(5):34-44
- [62] Zhu J, Li Y, Shen H. Numerical simulation of the wind field's impact on the expansion of the changjiang river diluted water in summer. *Oceanologia et Limnologia Sinica*. 1997;**28**(1):72-79
- [63] Zhu J, Xiao C, Shen H. Numerical model simulation of expansion of Changjiang diluted water in summer. *Acta Oceanologica Sinica*. 1998;**20**(5):13-22
- [64] Zhu C, Wang Z-H, Xue B, Yu P-S, Pan J-M, Wagner T, et al. Characterizing the depositional settings for sedimentary organic matter distributions in the Lower Yangtze River-East China Sea Shelf System. *Estuarine, Coastal and Shelf Science*. 2011;**93**(3):182-191

